EUROPEAN ORGANIZATION FOR NUCLEAR RESEARCH

CERN-EP/89-06
January 17th, 1989

A High Statistics Measurement of the Proton Structure Functions $F_2(x,Q^2)$ and R from Deep Inelastic Muon Scattering at High Q^2

BCDMS Collaboration

A.C. Benvenuti, D. Bollini, G. Bruni, T. Camporesi, L. Monari[1] and F.L. Navarria
Dipartimento di Fisica dell'Università and INFN, Bologna, Italy

A. Argento[2], J. Cvach[3], W. Lohmann[4], L. Piemontese[5] and P. Zavada[3]
CERN, Geneva, Switzerland

A.A. Akhundov, V.I. Genchev, I.A. Golutvin, Yu.T. Kiryushin, V.G. Krivokhizhin, V.V. Kukhtin, R. Lednicky, S. Nemecek, P. Reimer, I.A. Savin, G.I. Smirnov, J. Strachota[3], G. Sultanov[6], P. Todorov[6] and A.G. Volodko
Joint Institute for Nuclear Research, Dubna, USSR

D. Jamnik[7], R. Kopp[8], U. Meyer-Berkhout, A. Staude, K.-M. Teichert, R. Tirler[9], R. Voss[10] and C. Zupancic
Sektion Physik der Universität, München, Federal Republic of Germany[11]

M. Cribier, J. Feltesse, A. Milsztajn, A. Ouraou, P. Rich-Hennion, Y. Sacquin, G. Smadja and M. Virchaux
DPhPE, CEN Saclay, France

Abstract

We present results on a high statistics study of the proton structure functions $F_2(x,Q^2)$ and $R = \sigma_L/\sigma_T$ measured in deep inelastic scattering of muons on a hydrogen target. The analysis is based on $1.8 \cdot 10^6$ events after all cuts, recorded at beam energies of 100, 120, 200 and 280 GeV and covering a kinematic range $0.06 \leq x \leq 0.80$ and $7\ \text{GeV}^2 \leq Q^2 \leq 260\ \text{GeV}^2$. At small x, we find R to be different from zero in agreement with predictions of perturbative QCD.

Submitted to Physics Letters B

---

[1] Deceased.

[2] Now at Digital Equipment, Torino, Italy.

[3] On leave from Institute of Physics, CSAV, Prague, Czechoslovakia.

[4] On leave from the Institut für Hochenergiephysik der AdW der DDR, Berlin-Zeuthen, GDR.

[5] Now at INFN, Ferrara, Italy.

[6] Now at the Institute of Nuclear Research and Nuclear Energy, Bulgarian Academy of Sciences, Sofia, Bulgaria.

[7] On leave from E. Kardelj University and the J. Stefan Institute, Ljubljana, Yugoslavia.

[8] Now at Siemens AG, Munich, Germany.

[9] Now at DPhPE, CEN Saclay, France.

[10] Now at CERN, Geneva, Switzerland.

[11] Funded in part by the German Federal Minister for Research and Technology (BMFT) under contract number 054MU12P6.

We present results on the structure functions of the proton measured with high statistics in deep inelastic scattering of muons on a hydrogen target. In the one-photon exchange approximation, the deep inelastic muon-proton cross section can be written as

$$\frac{d^2\sigma}{dQ^2dx} = \frac{4\pi\alpha^2}{Q^4x} \cdot \left[1-y - \frac{Q^2}{4E^2} + \frac{y^2E^2+Q^2}{2E^2[R(x,Q^2)+1]} \right] \cdot F_2(x,Q^2) \qquad (1)$$

where E is the energy of the incident beam, Q^2 the squared four-momentum transfer between the muon and the proton, and x and y are the Bjorken scaling variables. This cross section depends on two structure functions F_2 and R, where $R = \sigma_L/\sigma_T$ is the ratio of absorption cross sections for virtual photons of longitudinal and transverse polarization. R is related to F_2 and to the longitudinal structure function F_L by

$$R(x,Q^2) = \frac{F_L(x,Q^2)}{(1+4M^2x^2/Q^2) \cdot F_2(x,Q^2) - F_L(x,Q^2)} \qquad (2)$$

where M is the mass of the proton.

The data were collected at the CERN SPS muon beam with a high-luminosity spectrometer which is described in more detail elsewhere [1]. It consists of a 40 m long segmented toroidal iron magnet which is magnetized close to saturation and surrounds a 30 m long "internal" liquid hydrogen target. The iron absorbs the hadronic shower after a few meters and the surviving scattered muon is focused towards the spectrometer axis. The toroids are instrumented with scintillation trigger counters and multiwire proportional chambers. A 10 m long "external" target in front of the spectrometer magnet extends the acceptance of the apparatus to smaller angles, i.e. to smaller values of x and Q^2, than are accessible with the internal target. Four hodoscopes along the spectrometer axis detect the incoming muons and measure their trajectories. The momentum of the incident muon is measured with a spectrometer consisting of an air-gap magnet and another four scintillator hodoscopes upstream of the apparatus.

The results presented here are based on $1.8 \cdot 10^6$ reconstructed events after all cuts, recorded with positive muon beams of 100, 120, 200 and 280 GeV energy. The kinematic ranges and data samples

are summarized in Table 1. The data analysis is similar to the one performed by our collaboration in an earlier experiment using a carbon target [2,3,4]. A more detailed account of this analysis can be found in ref. [5]. The principal difference between this and the carbon target experiment is due to the additional external target. For events originating from the internal target, the geometrical acceptance is greater than 65% and is rather flat in the kinematic region $x > 0.25$ and $Q^2/2ME > 0.10$. For events from the external target, the acceptance depends on the position of the interaction vertex along the beam direction; only data points with an acceptance larger than 50% were retained for the analysis. The structure functions were evaluated separately for the two target regions. The background from target wall interactions was determined from special empty target runs and was subtracted from the data. At all beam energies, the data from external and internal target were found to be in statistical agreement and were combined for the subsequent analysis. Radiative corrections were applied using the calculations of refs. [6]. The error on $F_2(x,Q^2)$ from uncertainties on these corrections is estimated to be smaller than 1%.

The principal sources of systematic errors in the data are uncertainties in:

- the calibration of the incident beam energy ($\Delta E/E < 0.15\%$),
- the calibration of the spectrometer magnetic field ($\Delta B/B < 0.15\%$),
- corrections for the energy loss ϵ of muons in iron [7] ($\Delta\epsilon/\epsilon < 1\%$),
- corrections for the finite resolution Σ of the spectrometer ($\Delta\Sigma/\Sigma < 5\%$),
- the relative cross section normalization of data taken at different beam energies (1%),
- the absolute cross section normalization (3%).

Most of the results presented in this and a following paper [8], especially those on R and on the comparison of scaling violations to QCD predictions, are affected by the uncertainty on the relative but not on the absolute cross section normalization. Systematic errors originating from uncertainties in the detector efficiencies (0.5%) are small due to the redundancy in the experimental apparatus. A detailed discussion of the Monte Carlo simulation used to compute the acceptance and the resolution of the apparatus, of the treatment of the systematic errors, and of the calibrations undertaken to minimize them can be found in refs. [2,5].

According to equation (1) the measured cross section depends on the two functions $R = \sigma_L/\sigma_T$ and F_2. Both functions can be separated by comparing cross sections at the same value of x and Q^2, measured at different beam energies. In this analysis we have chosen to compare the values of four test F_2's, called $F_2^*(R)$, obtained at the four beam energies assuming trial values for R. The experimental value of R was then obtained together with the parameters of a common phenomenological parametrization of F_2 by minimizing the χ^2 of the four $F_2^*(R)$ with respect to this parametrization. This was done separately in each bin of x under the assumption that R (eq. 2) is independent of Q^2 in our kinematic range, as suggested by QCD calculations which predict only a weak (logarithmic) variation of the longitudinal structure function F_L with Q^2 [9]

$$F_L(x,Q^2) = \frac{\alpha_s(Q^2)}{2\pi} \cdot x^2 \cdot \int_x^1 \left[\frac{8}{3}F_2(z,Q^2) + \frac{40}{9}\left(1-\frac{x}{z}\right) zG(z,Q^2)\right] \cdot \frac{dz}{z^3} \qquad (3)$$

where $\alpha_s(Q^2)$ is the running coupling constant of QCD. The theoretical prediction R_{QCD} was computed from equations (2) and (3) assuming a gluon momentum distribution $xG(x,Q_0^2) = 4.5\cdot(1-x)^8$ at $Q_0^2 = 5\ GeV^2$ and a QCD mass scale parameter $\Lambda = 220$ MeV [8]. In the kinematic range of our experiment, this prediction does not depend strongly on the gluon distribution assumed. Equation (3) does not account for effects of the charm quark mass and for target mass corrections which were included following refs. [10] and [11] respectively. The experimental results for R are given in Table 2 and are compared to the QCD prediction in Fig. 1 together with earlier hydrogen data in a similar kinematical range by the European Muon Collaboration (EMC) [12]. At $x > 0.20$, the measured values are compatible with zero in agreement with our carbon target measurement [2]. At smaller x, the data show a rise which is consistent with the QCD prediction.

R_{QCD} was used to compute the final structure functions at the four different beam energies which are given in Tables 3 – 6 and are shown in Fig. 2. The agreement between the different data sets in the region of large x allows to set stringent limits on most of the systematic errors as is discussed in more detail in ref. [2]. The final $F_2(x,Q^2)$ from the combined data sets is shown in Fig. 3. The scaling violations which are observed in these data are compared to predictions from perturbative QCD in a separate paper [8].

Also shown in Fig. 3 are the earlier EMC data from muon-hydrogen scattering [12] and the SLAC-MIT results from electron-hydrogen scattering at lower Q^2 [13]. The x dependence of F_2 from this experiment is compared to the EMC result in Fig. 4 where the data are averaged over the Q^2 range common to both measurements. The agreement is poor, especially at small x where F_2 measured in the present experiment is larger by up to 15%. In the lowest bin of x, about 4% of this difference is due to the fact that the EMC result was obtained using $R = 0$. A similar behaviour was observed in our measurement on a carbon target [2] which indicated a steeper x dependence of F_2 than measured in earlier experiments. A quantitative comparison to the SLAC data is difficult since the experiments cover disjoint ranges of Q^2.

In conclusion, we have presented a high statistics measurement of the proton structure functions F_2 and R from deep inelastic scattering of muons at high Q^2 on a hydrogen target. The systematic uncertainties are comparable to the statistical accuracy of the results. $R = \sigma_L/\sigma_T$ is found to be in good agreement with the perturbative QCD prediction.

References

[1] BCDMS, D. Bollini et al., Nucl. Instr. Meth. 204 (1983) 333;
BCDMS, A.C. Benvenuti et al., Nucl. Instr. Meth. 226 (1984) 330.

[2] BCDMS, A.C. Benvenuti et al., Phys. Lett. 195B (1987) 91.

[3] BCDMS, A.C. Benvenuti et al., Phys. Lett. 195B (1987) 97.

[4] M. Virchaux, Thèse, Université Paris VII, 1988.

[5] A. Ouraou, Thèse, Université Paris XI, 1988.

[6] A.A. Akhundov et al., Sov. J. Nucl. Phys. 26 (1977) 660;
D.Yu. Bardin and N.M. Shumeiko, Sov. J. Nucl. Phys. 29 (1979) 499;
A.A. Akhundov et al., Sov. J. Nucl. Phys. 44 (1986) 988;
A.A. Akhundov et al., JINR Communication E2-86-104, Dubna 1986.

[7] BCDMS, R. Kopp et al., Z. Phys. C 28 (1985) 171;
W. Lohmann, R. Kopp and R. Voss, CERN 85-03 (CERN Yellow Report).

[8] BCDMS, A.C. Benvenuti et al., CERN-EP/89-07, submitted to Physics Letters B.

[9] G. Altarelli and G. Martinelli, Phys. Lett. 76B (1978) 89.

[10] M. Glück, E. Hoffmann and E. Reya, Z. Phys. C 13 (1982) 119.

[11] H. Georgi and D. Politzer, Phys. Rev. D14 (1976) 1829.

[12] EMC, J.J. Aubert et al., Nucl. Phys. B259 (1985) 189.

[13] A. Bodek et al., Phys. Rev. D20 (1979) 1471.

Table Captions

Table 1: Kinematic ranges and number of events after all cuts at the four beam energies.

Table 2: Results for $R = \sigma_L/\sigma_T$ as a function of x. R is assumed to be independent of Q^2 in each bin of x.

Table 3: $F_2(x,Q^2)$ measured at 100 GeV beam energy. The average beam energy at the interaction vertex is $<E> = 99.1$ GeV. Q^2 is given in GeV^2. $F_2(x,Q^2)$ is given both for $R = \sigma_L/\sigma_T = 0$ (F_2^0) and for $R = R_{QCD}$ (F_2^1). The statistical error ΔF_2 applies to F_2^0 and can be scaled to apply to F_2^1. The systematic errors are given as multiplicative factors to be applied to $F_2(x,Q^2)$: f_b, f_s and f_r are the uncertainties due to beam momentum calibration, spectrometer magnetic field calibration and spectrometer resolution, respectively; f_d is the systematic error due to detector and trigger inefficiencies and f_n is due to the uncertainty in the relative normalization of data from external and internal targets. The overall normalization uncertainty discussed in the text is not shown here.

Table 4: As Table 3, for the measurement at 120 GeV beam energy. The average beam energy at the interaction vertex is $<E> = 117.9$ GeV.

Table 5: As Table 3, for the measurement at 200 GeV beam energy. The average beam energy at the interaction vertex is $<E> = 196.3$ GeV.

Table 6: As Table 3, for the measurement at 280 GeV beam energy. The average beam energy at the interaction vertex is $<E> = 277.0$ GeV.

Table 1: The data sample

Beam energy (GeV)	Q^2 range (GeV^2)	x range	Number of events
100	7- 80	0.06-0.80	530 000
120	8-106	0.06-0.80	330 000
200	16-150	0.06-0.80	770 000
280	30-260	0.08-0.80	180 000

Table 2: Results for $R = \sigma_L/\sigma_T$

x	$<Q^2>$ (GeV^2)	R	statistical error	systematic error
0.07	15	0.167	0.134	0.074
0.10	20	0.122	0.078	0.062
0.14	20	0.163	0.055	0.040
0.18	25	0.121	0.051	0.031
0.225	30	0.046	0.032	0.028
0.275	35	0.025	0.027	0.022
0.35	40	0.023	0.025	0.022
0.45	45	−0.011	0.035	0.027
0.55	50	0.005	0.056	0.039
0.65	50	−0.057	0.092	0.071

Table 3: $F_2(x,Q^2)$ at 100 GeV beam energy

x	Q^2	F_2^0	ΔF_2	F_2^1	f_b	f_s	f_r	f_d	f_n
0.07	7.50	0.38934	0.00600	0.40205	0.997	0.999	1.001	1.015	1.010
	8.75	0.37624	0.00521	0.39363	0.997	0.999	1.013	1.015	1.010
0.10	7.50	0.38055	0.00424	0.38468	0.996	0.997	1.003	1.005	1.010
	8.75	0.38347	0.00351	0.38926	0.997	0.998	1.007	1.005	1.010
	10.25	0.37960	0.00362	0.38772	0.997	0.999	1.007	1.005	1.010
0.14	8.75	0.37560	0.00390	0.37768	0.996	0.997	1.002	1.000	1.010
	10.25	0.37676	0.00396	0.37965	0.996	0.997	1.004	1.000	1.010
	11.75	0.37259	0.00430	0.37641	0.997	0.998	1.006	1.000	1.010
	13.25	0.36575	0.00468	0.37062	0.997	0.998	1.002	1.000	1.010
	15.00	0.37196	0.00481	0.37847	0.997	0.999	1.005	1.000	1.010
0.18	8.75	0.36786	0.00489	0.36886	0.995	0.996	0.995	1.000	1.010
	10.25	0.36457	0.00474	0.36592	0.996	0.997	1.001	1.000	1.010
	11.75	0.36492	0.00501	0.36670	0.996	0.997	1.002	1.000	1.010
	13.25	0.36270	0.00534	0.36497	0.996	0.998	1.005	1.000	1.010
	15.00	0.36228	0.00521	0.36523	0.997	0.998	1.003	1.000	1.010
	17.00	0.35350	0.00571	0.35727	0.997	0.999	0.998	1.000	1.010
0.225	10.25	0.34051	0.00481	0.34120	0.995	0.997	0.999	1.000	1.010
	11.75	0.34545	0.00501	0.34635	0.996	0.997	1.000	1.000	1.010
	13.25	0.33693	0.00520	0.33805	0.996	0.998	1.001	1.000	1.010
	15.00	0.33517	0.00490	0.33659	0.996	0.998	0.999	1.000	1.010
	17.00	0.31962	0.00522	0.32138	0.997	0.999	1.002	1.000	1.010
	19.00	0.32172	0.00578	0.32395	0.997	0.999	1.004	1.000	1.010
	21.50	0.31154	0.00552	0.31436	0.997	0.999	1.003	1.000	1.010
	24.50	0.32112	0.00522	0.32498	0.997	1.000	0.999	1.000	1.000
	28.00	0.31410	0.00529	0.31917	0.997	1.000	1.003	1.000	1.000
0.275	10.25	0.30440	0.00536	0.30476	0.996	0.998	0.987	1.000	1.010
	11.75	0.29925	0.00545	0.29971	0.996	0.998	0.994	1.000	1.010
	13.25	0.30155	0.00574	0.30213	0.996	0.999	0.997	1.000	1.010
	15.00	0.30341	0.00527	0.30414	0.997	0.999	0.998	1.000	1.010
	17.00	0.30373	0.00564	0.30467	0.997	0.999	0.999	1.000	1.010
	19.00	0.28923	0.00592	0.29035	0.997	1.000	0.997	1.000	1.010
	21.50	0.29763	0.00559	0.29911	0.997	1.000	0.999	1.000	1.010
	24.50	0.27886	0.00498	0.28068	0.997	1.000	1.000	1.000	1.000
	28.00	0.28971	0.00507	0.29223	0.997	1.000	1.004	1.000	1.000
	32.50	0.28090	0.00471	0.28428	0.998	1.001	1.003	1.000	1.000
	37.50	0.26784	0.00583	0.27224	0.998	1.001	1.002	1.000	1.000
0.35	11.75	0.24001	0.00427	0.24021	0.998	1.002	0.988	1.000	1.010
	13.25	0.23349	0.00434	0.23373	0.998	1.002	0.991	1.000	1.010
	15.00	0.23093	0.00383	0.23122	0.998	1.002	0.993	1.000	1.010
	17.00	0.23689	0.00410	0.23727	0.998	1.002	0.995	1.000	1.010
	19.00	0.22257	0.00416	0.22300	0.998	1.002	0.996	1.000	1.010
	21.50	0.23218	0.00388	0.23275	0.998	1.002	0.998	1.000	1.010
	24.50	0.22318	0.00283	0.22389	0.998	1.002	0.997	1.000	1.004
	28.00	0.22454	0.00353	0.22548	0.998	1.002	0.996	1.000	1.000
	32.50	0.21917	0.00320	0.22042	0.998	1.002	1.002	1.000	1.000
	37.50	0.21761	0.00344	0.21929	0.998	1.002	0.999	1.000	1.000
	43.00	0.21422	0.00367	0.21644	0.998	1.002	1.000	1.000	1.000

0.45	11.75	0.16020	0.00409	0.16027	1.004	1.012	1.002	1.000	1.010
	13.25	0.15598	0.00430	0.15606	1.003	1.011	0.995	1.000	1.010
	15.00	0.15493	0.00378	0.15503	1.003	1.010	0.994	1.000	1.010
	17.00	0.15323	0.00403	0.15335	1.002	1.009	0.999	1.000	1.010
	19.00	0.15558	0.00429	0.15573	1.001	1.008	1.004	1.000	1.010
	21.50	0.14470	0.00362	0.14488	1.001	1.008	0.996	1.000	1.010
	24.50	0.14443	0.00256	0.14465	1.000	1.007	0.998	1.000	1.004
	28.00	0.13996	0.00313	0.14024	1.000	1.006	0.997	1.000	1.000
	32.50	0.14332	0.00282	0.14370	0.999	1.006	0.996	1.000	1.000
	37.50	0.14506	0.00310	0.14557	0.999	1.005	0.998	1.000	1.000
	43.00	0.14063	0.00311	0.14129	0.999	1.005	0.996	1.000	1.000
	49.50	0.13379	0.00310	0.13463	0.999	1.005	0.998	1.000	1.000
	57.00	0.13603	0.00354	0.13718	0.998	1.004	0.998	1.000	1.000
0.55	11.75	0.09286	0.00316	0.09289	1.016	1.031	1.021	1.000	1.010
	13.25	0.08784	0.00329	0.08787	1.014	1.028	1.015	1.000	1.010
	15.00	0.08998	0.00306	0.09002	1.012	1.025	1.012	1.000	1.010
	17.00	0.08469	0.00308	0.08473	1.010	1.023	1.008	1.000	1.010
	19.00	0.08286	0.00319	0.08291	1.008	1.021	1.006	1.000	1.010
	21.50	0.08279	0.00289	0.08285	1.007	1.018	1.003	1.000	1.010
	24.50	0.08513	0.00206	0.08520	1.005	1.017	1.006	1.000	1.004
	28.00	0.08099	0.00199	0.08108	1.004	1.015	1.008	1.000	1.004
	32.50	0.08516	0.00236	0.08528	1.003	1.013	1.005	1.000	1.000
	37.50	0.08100	0.00247	0.08115	1.002	1.012	1.002	1.000	1.000
	43.00	0.08005	0.00251	0.08024	1.001	1.010	1.000	1.000	1.000
	49.50	0.07690	0.00250	0.07715	1.000	1.009	0.999	1.000	1.000
	57.00	0.07387	0.00267	0.07418	1.000	1.009	0.999	1.000	1.000
	65.50	0.07196	0.00287	0.07237	0.999	1.008	0.998	1.000	1.000
0.65	13.25	0.04389	0.00187	0.04390	1.034	1.060	1.084	1.000	1.010
	15.00	0.04264	0.00166	0.04265	1.030	1.054	1.071	1.000	1.010
	17.00	0.04166	0.00184	0.04167	1.026	1.048	1.063	1.000	1.010
	19.00	0.04150	0.00198	0.04151	1.022	1.044	1.052	1.000	1.010
	21.50	0.04010	0.00178	0.04012	1.018	1.039	1.044	1.000	1.010
	24.50	0.04115	0.00121	0.04117	1.015	1.035	1.028	1.000	1.003
	28.00	0.03869	0.00121	0.03871	1.013	1.031	1.026	1.000	1.003
	32.50	0.03826	0.00143	0.03829	1.010	1.027	1.021	1.000	1.000
	37.50	0.03662	0.00161	0.03666	1.008	1.024	1.015	1.000	1.000
	43.00	0.03524	0.00166	0.03529	1.006	1.021	1.011	1.000	1.000
	49.50	0.03303	0.00166	0.03309	1.004	1.019	1.008	1.000	1.000
	57.00	0.03363	0.00184	0.03371	1.003	1.017	1.006	1.000	1.000
	65.50	0.02980	0.00186	0.02989	1.002	1.015	1.005	1.000	1.000
	75.00	0.03194	0.00217	0.03206	1.001	1.014	1.003	1.000	1.000
0.75	24.50	0.01357	0.00064	0.01357	1.040	1.076	1.088	1.000	1.000
	28.00	0.01365	0.00068	0.01366	1.033	1.067	1.072	1.000	1.000
	32.50	0.01307	0.00065	0.01308	1.027	1.059	1.064	1.000	1.000
	37.50	0.01169	0.00074	0.01170	1.022	1.052	1.051	1.000	1.000
	43.00	0.01105	0.00079	0.01106	1.018	1.046	1.046	1.000	1.000
	49.50	0.01082	0.00084	0.01083	1.014	1.040	1.037	1.000	1.000
	57.00	0.01148	0.00100	0.01149	1.011	1.036	1.025	1.000	1.000
	65.50	0.00966	0.00102	0.00968	1.008	1.032	1.021	1.000	1.000
	75.00	0.01031	0.00119	0.01033	1.006	1.028	1.017	1.000	1.000

Table 4: $F_2(x,Q^2)$ at 120 GeV beam energy

x	Q^2	F_2^0	ΔF_2	F_2^1	f_b	f_s	f_r	f_d	f_n
0.07	8.75	0.37824	0.00583	0.38956	0.997	0.999	1.003	1.015	1.010
	10.25	0.37381	0.00596	0.38982	0.997	0.999	1.008	1.015	1.010
0.10	10.25	0.38707	0.00456	0.39249	0.997	0.998	1.005	1.005	1.010
	11.75	0.38341	0.00476	0.39066	0.997	0.998	1.006	1.005	1.010
	13.25	0.38291	0.00516	0.39239	0.997	0.999	1.004	1.005	1.010
0.14	11.75	0.38246	0.00571	0.38505	0.996	0.997	1.002	1.000	1.010
	13.25	0.37607	0.00583	0.37936	0.996	0.998	1.004	1.000	1.010
	15.00	0.37557	0.00564	0.37987	0.997	0.998	1.004	1.000	1.010
	17.00	0.37197	0.00627	0.37759	0.997	0.999	1.002	1.000	1.010
	19.00	0.36233	0.00684	0.36935	0.997	0.999	1.000	1.000	1.010
0.18	11.75	0.36009	0.00686	0.36127	0.995	0.997	0.998	1.000	1.010
	13.25	0.35608	0.00688	0.35757	0.996	0.997	1.000	1.000	1.010
	15.00	0.34792	0.00643	0.34979	0.996	0.998	1.002	1.000	1.010
	17.00	0.35021	0.00693	0.35267	0.997	0.998	1.003	1.000	1.010
	19.00	0.34539	0.00745	0.34847	0.997	0.999	1.003	1.000	1.010
	21.50	0.35670	0.00694	0.36087	0.997	0.999	1.002	1.000	1.010
	24.50	0.33272	0.00798	0.33792	0.997	0.999	1.000	1.000	1.010
0.225	11.75	0.32274	0.00660	0.32331	0.995	0.997	1.002	1.000	1.010
	13.25	0.34040	0.00703	0.34116	0.996	0.997	1.002	1.000	1.010
	15.00	0.32526	0.00632	0.32619	0.996	0.998	1.001	1.000	1.010
	17.00	0.33403	0.00678	0.33525	0.996	0.998	1.000	1.000	1.010
	19.00	0.31631	0.00705	0.31776	0.997	0.999	1.002	1.000	1.010
	21.50	0.32392	0.00648	0.32585	0.997	0.999	1.003	1.000	1.010
	24.50	0.31374	0.00709	0.31622	0.997	0.999	1.001	1.000	1.010
	28.00	0.31301	0.00592	0.31632	0.997	1.000	1.003	1.000	1.000
	32.50	0.31897	0.00582	0.32366	0.997	1.000	1.002	1.000	1.000
0.275	13.25	0.30041	0.00785	0.30080	0.996	0.998	1.003	1.000	1.010
	15.00	0.31094	0.00731	0.31145	0.996	0.999	1.006	1.000	1.010
	17.00	0.29574	0.00722	0.29635	0.997	0.999	1.002	1.000	1.010
	19.00	0.29560	0.00754	0.29636	0.997	0.999	1.005	1.000	1.010
	21.50	0.29235	0.00676	0.29332	0.997	1.000	1.000	1.000	1.010
	24.50	0.28614	0.00484	0.28738	0.997	1.000	1.003	1.000	1.004
	28.00	0.28387	0.00463	0.28549	0.997	1.000	0.998	1.000	1.004
	32.50	0.28255	0.00472	0.28478	0.997	1.000	1.001	1.000	1.002
	37.50	0.28359	0.00609	0.28665	0.998	1.001	1.004	1.000	1.000
	43.00	0.26798	0.00615	0.27188	0.998	1.001	1.006	1.000	1.000
0.35	13.25	0.23697	0.00604	0.23713	0.998	1.002	1.006	1.000	1.010
	15.00	0.23426	0.00545	0.23446	0.998	1.002	1.006	1.000	1.010
	17.00	0.23448	0.00534	0.23473	0.998	1.002	1.001	1.000	1.010
	19.00	0.22909	0.00549	0.22939	0.998	1.002	1.004	1.000	1.010
	21.50	0.22136	0.00466	0.22173	0.998	1.002	0.997	1.000	1.010
	24.50	0.23127	0.00351	0.23176	0.998	1.002	1.004	1.000	1.004
	28.00	0.22575	0.00332	0.22638	0.998	1.002	1.003	1.000	1.004
	32.50	0.22033	0.00319	0.22116	0.998	1.002	1.000	1.000	1.003
	37.50	0.22098	0.00413	0.22210	0.998	1.002	1.000	1.000	1.000
	43.00	0.21710	0.00418	0.21858	0.998	1.002	1.004	1.000	1.000
	49.50	0.20737	0.00422	0.20928	0.998	1.002	1.001	1.000	1.000

	57.00	0.21152	0.00496	0.21417	0.998	1.002	1.004	1.000	1.000
0.45	13.25	0.15958	0.00593	0.15964	1.005	1.013	1.003	1.000	1.010
	15.00	0.16145	0.00548	0.16152	1.004	1.012	0.997	1.000	1.010
	17.00	0.15240	0.00528	0.15248	1.003	1.011	0.996	1.000	1.010
	19.00	0.15374	0.00554	0.15384	1.002	1.010	1.007	1.000	1.010
	21.50	0.15342	0.00480	0.15355	1.002	1.009	1.002	1.000	1.010
	24.50	0.14968	0.00319	0.14984	1.001	1.008	1.000	1.000	1.004
	28.00	0.14585	0.00303	0.14605	1.000	1.007	1.003	1.000	1.004
	32.50	0.14579	0.00291	0.14605	1.000	1.006	0.999	1.000	1.003
	37.50	0.14296	0.00316	0.14330	0.999	1.006	0.999	1.000	1.002
	43.00	0.14187	0.00365	0.14231	0.999	1.005	1.004	1.000	1.000
	49.50	0.13688	0.00367	0.13745	0.999	1.005	1.003	1.000	1.000
	57.00	0.13681	0.00386	0.13757	0.999	1.005	1.007	1.000	1.000
	65.50	0.13381	0.00421	0.13481	0.998	1.004	1.002	1.000	1.000
	75.00	0.12253	0.00479	0.12375	0.998	1.004	1.000	1.000	1.000
0.55	15.00	0.08494	0.00385	0.08496	1.015	1.030	1.018	1.000	1.010
	17.00	0.07999	0.00362	0.08002	1.013	1.027	1.015	1.000	1.010
	19.00	0.09073	0.00451	0.09077	1.011	1.024	1.006	1.000	1.010
	21.50	0.08537	0.00371	0.08541	1.009	1.022	1.007	1.000	1.010
	24.50	0.09156	0.00433	0.09161	1.007	1.019	1.006	1.000	1.010
	28.00	0.08154	0.00229	0.08160	1.006	1.017	1.006	1.000	1.004
	32.50	0.07923	0.00220	0.07931	1.004	1.015	1.003	1.000	1.003
	37.50	0.07860	0.00247	0.07870	1.003	1.014	1.004	1.000	1.002
	43.00	0.07617	0.00285	0.07629	1.002	1.012	1.004	1.000	1.000
	49.50	0.07888	0.00300	0.07905	1.001	1.011	1.003	1.000	1.000
	57.00	0.07464	0.00309	0.07485	1.001	1.010	1.001	1.000	1.000
	65.50	0.06671	0.00320	0.06696	1.000	1.009	1.000	1.000	1.000
	75.00	0.07039	0.00357	0.07074	0.999	1.008	0.999	1.000	1.000
	86.00	0.07020	0.00379	0.07066	0.999	1.007	1.002	1.000	1.000
0.65	17.00	0.04111	0.00214	0.04112	1.032	1.057	1.069	1.000	1.010
	19.00	0.04282	0.00238	0.04283	1.028	1.052	1.059	1.000	1.010
	21.50	0.04106	0.00218	0.04107	1.024	1.046	1.055	1.000	1.010
	24.50	0.03654	0.00230	0.03655	1.020	1.041	1.046	1.000	1.010
	28.00	0.03692	0.00225	0.03694	1.017	1.037	1.038	1.000	1.010
	32.50	0.03679	0.00136	0.03681	1.013	1.032	1.028	1.000	1.003
	37.50	0.04065	0.00170	0.04068	1.011	1.028	1.022	1.000	1.002
	43.00	0.03612	0.00184	0.03615	1.009	1.025	1.018	1.000	1.000
	49.50	0.03589	0.00198	0.03593	1.007	1.022	1.015	1.000	1.000
	57.00	0.03042	0.00193	0.03047	1.005	1.020	1.011	1.000	1.000
	65.50	0.03560	0.00231	0.03567	1.003	1.018	1.010	1.000	1.000
	75.00	0.03168	0.00243	0.03176	1.002	1.016	1.008	1.000	1.000
	86.00	0.03041	0.00251	0.03051	1.001	1.014	1.009	1.000	1.000
	99.00	0.03436	0.00295	0.03451	1.000	1.013	1.006	1.000	1.000
0.75	32.50	0.01335	0.00075	0.01335	1.035	1.070	1.075	1.000	1.000
	37.50	0.01194	0.00084	0.01194	1.029	1.061	1.068	1.000	1.000
	43.00	0.01238	0.00091	0.01239	1.024	1.054	1.061	1.000	1.000
	49.50	0.01155	0.00097	0.01156	1.019	1.048	1.054	1.000	1.000
	57.00	0.01169	0.00105	0.01170	1.015	1.042	1.046	1.000	1.000
	65.50	0.01056	0.00117	0.01057	1.012	1.037	1.041	1.000	1.000
	75.00	0.00992	0.00124	0.00993	1.009	1.033	1.030	1.000	1.000
	86.00	0.00961	0.00134	0.00963	1.006	1.029	1.026	1.000	1.000
	99.00	0.00815	0.00131	0.00817	1.004	1.026	1.020	1.000	1.000

Table 5: $F_2(x,Q^2)$ at 200 GeV beam energy

x	Q^2	F_2^0	ΔF_2	F_2^1	f_b	f_s	f_r	f_d	f_n
0.07	17.00	0.39928	0.00521	0.41459	0.997	0.999	0.996	1.015	1.005
	19.00	0.39989	0.00527	0.41972	0.998	1.000	1.005	1.015	1.005
0.10	19.00	0.39548	0.00407	0.40180	0.997	0.999	1.004	1.005	1.005
	21.50	0.39338	0.00317	0.40171	0.997	0.999	1.006	1.005	1.005
	24.50	0.39402	0.00339	0.40528	0.997	0.999	1.003	1.005	1.005
0.14	21.50	0.37841	0.00361	0.38121	0.996	0.998	1.005	1.000	1.005
	24.50	0.37991	0.00378	0.38366	0.997	0.998	1.007	1.000	1.005
	28.00	0.37499	0.00362	0.37999	0.997	0.999	1.003	1.000	1.005
	32.50	0.36709	0.00356	0.37396	0.997	0.999	1.004	1.000	1.005
0.18	21.50	0.35061	0.00419	0.35183	0.996	0.997	1.005	1.000	1.005
	24.50	0.36077	0.00434	0.36243	0.996	0.998	1.002	1.000	1.005
	28.00	0.36004	0.00413	0.36224	0.997	0.998	1.003	1.000	1.005
	32.50	0.34712	0.00288	0.35007	0.997	0.999	1.004	1.000	1.003
	37.50	0.34052	0.00302	0.34450	0.997	0.999	0.998	1.000	1.002
	43.00	0.34255	0.00301	0.34801	0.997	1.000	1.001	1.000	1.002
0.225	28.00	0.32246	0.00384	0.32347	0.996	0.998	0.997	1.000	1.005
	32.50	0.32715	0.00365	0.32855	0.997	0.999	1.002	1.000	1.005
	37.50	0.31302	0.00276	0.31485	0.997	0.999	0.999	1.000	1.002
	43.00	0.31337	0.00269	0.31585	0.997	1.000	1.003	1.000	1.002
	49.50	0.30607	0.00264	0.30939	0.997	1.000	1.005	1.000	1.002
	57.00	0.31349	0.00363	0.31816	0.998	1.000	1.003	1.000	1.000
0.275	28.00	0.28822	0.00409	0.28872	0.997	0.999	1.003	1.000	1.005
	32.50	0.28252	0.00372	0.28319	0.997	1.000	0.996	1.000	1.005
	37.50	0.27908	0.00290	0.27997	0.997	1.000	1.000	1.000	1.003
	43.00	0.27264	0.00272	0.27380	0.997	1.000	0.998	1.000	1.002
	49.50	0.27001	0.00272	0.27157	0.997	1.000	1.004	1.000	1.002
	57.00	0.27276	0.00292	0.27491	0.997	1.001	1.001	1.000	1.002
	65.50	0.26985	0.00361	0.27275	0.998	1.001	1.004	1.000	1.000
	75.00	0.26068	0.00385	0.26446	0.998	1.001	1.007	1.000	1.000
0.35	32.50	0.22221	0.00276	0.22247	0.998	1.002	0.998	1.000	1.005
	37.50	0.21985	0.00209	0.22019	0.998	1.002	1.002	1.000	1.003
	43.00	0.21666	0.00201	0.21710	0.998	1.002	1.004	1.000	1.002
	49.50	0.21473	0.00196	0.21531	0.998	1.002	1.003	1.000	1.002
	57.00	0.21410	0.00203	0.21488	0.998	1.002	1.005	1.000	1.002
	65.50	0.20758	0.00210	0.20861	0.998	1.002	0.998	1.000	1.001
	75.00	0.20193	0.00258	0.20327	0.998	1.002	1.001	1.000	1.000
	86.00	0.20554	0.00273	0.20739	0.998	1.002	1.006	1.000	1.000
	99.00	0.20033	0.00297	0.20279	0.998	1.002	1.003	1.000	1.000
0.45	32.50	0.14298	0.00266	0.14306	1.002	1.010	1.006	1.000	1.005
	37.50	0.13689	0.00276	0.13699	1.002	1.009	1.003	1.000	1.005
	43.00	0.13873	0.00183	0.13886	1.001	1.008	1.004	1.000	1.002
	49.50	0.13676	0.00179	0.13693	1.000	1.007	1.001	1.000	1.002
	57.00	0.13594	0.00185	0.13616	1.000	1.006	0.997	1.000	1.002
	65.50	0.13030	0.00183	0.13059	0.999	1.006	1.003	1.000	1.002
	75.00	0.12735	0.00225	0.12772	0.999	1.005	1.002	1.000	1.000
	86.00	0.13085	0.00235	0.13136	0.999	1.005	1.005	1.000	1.000

	99.00	0.12724	0.00243	0.12791	0.999	1.005	1.000	1.000	1.000
	115.50	0.12334	0.00239	0.12426	0.998	1.004	1.003	1.000	1.000
0.55	32.50	0.07733	0.00202	0.07735	1.011	1.025	1.021	1.000	1.005
	37.50	0.08019	0.00227	0.08022	1.009	1.022	1.017	1.000	1.005
	43.00	0.07591	0.00135	0.07595	1.007	1.019	1.012	1.000	1.002
	49.50	0.07558	0.00136	0.07563	1.006	1.017	1.011	1.000	1.002
	57.00	0.07589	0.00145	0.07595	1.004	1.015	1.006	1.000	1.002
	65.50	0.07090	0.00142	0.07098	1.003	1.013	1.002	1.000	1.001
	75.00	0.07022	0.00155	0.07032	1.002	1.012	1.002	1.000	1.001
	86.00	0.07299	0.00191	0.07313	1.001	1.011	1.004	1.000	1.000
	99.00	0.06683	0.00188	0.06700	1.000	1.010	1.001	1.000	1.000
	115.50	0.06513	0.00185	0.06536	1.000	1.009	1.000	1.000	1.000
	137.50	0.06621	0.00196	0.06655	0.999	1.008	1.003	1.000	1.000
0.65	32.50	0.03721	0.00122	0.03722	1.028	1.053	1.052	1.000	1.005
	37.50	0.03407	0.00130	0.03408	1.024	1.046	1.049	1.000	1.005
	43.00	0.03538	0.00078	0.03539	1.019	1.041	1.041	1.000	1.001
	49.50	0.03512	0.00083	0.03513	1.016	1.036	1.036	1.000	1.001
	57.00	0.03327	0.00086	0.03329	1.013	1.032	1.027	1.000	1.001
	65.50	0.03248	0.00092	0.03250	1.011	1.028	1.019	1.000	1.001
	75.00	0.03213	0.00100	0.03215	1.008	1.025	1.012	1.000	1.001
	86.00	0.03359	0.00126	0.03362	1.006	1.022	1.009	1.000	1.000
	99.00	0.03080	0.00128	0.03084	1.005	1.020	1.010	1.000	1.000
	115.50	0.02839	0.00125	0.02844	1.003	1.017	1.007	1.000	1.000
	137.50	0.02780	0.00130	0.02787	1.001	1.015	1.004	1.000	1.000
0.75	43.00	0.01252	0.00042	0.01252	1.048	1.090	1.110	1.000	1.000
	49.50	0.01189	0.00044	0.01189	1.041	1.079	1.099	1.000	1.000
	57.00	0.01076	0.00046	0.01076	1.034	1.070	1.092	1.000	1.000
	65.50	0.01068	0.00052	0.01068	1.028	1.061	1.084	1.000	1.000
	75.00	0.01117	0.00058	0.01117	1.024	1.054	1.078	1.000	1.000
	86.00	0.00999	0.00058	0.01000	1.018	1.048	1.066	1.000	1.000
	99.00	0.00905	0.00060	0.00906	1.015	1.042	1.059	1.000	1.000
	115.50	0.00813	0.00061	0.00814	1.011	1.037	1.048	1.000	1.000
	137.50	0.00903	0.00068	0.00904	1.007	1.032	1.037	1.000	1.000

Table 6: $F_2(x,Q^2)$ at 280 GeV beam energy

x	Q^2	F_2^0	ΔF_2	F_2^1	f_b	f_s	f_r	f_d	f_n
0.10	32.50	0.39629	0.00559	0.40558	0.997	0.999	1.008	1.005	1.005
	37.50	0.39408	0.00630	0.40695	0.998	1.000	1.004	1.005	1.005
0.14	37.50	0.37285	0.00654	0.37701	0.997	0.999	1.005	1.000	1.005
	43.00	0.37063	0.00645	0.37628	0.997	0.999	1.004	1.000	1.005
	49.50	0.35668	0.00661	0.36420	0.997	1.000	1.004	1.000	1.005
	57.00	0.37001	0.00802	0.38075	0.998	1.000	1.004	1.000	1.005
0.18	37.50	0.34630	0.00695	0.34807	0.996	0.998	0.998	1.000	1.005
	43.00	0.35894	0.00694	0.36142	0.997	0.999	0.999	1.000	1.005
	49.50	0.33701	0.00706	0.34020	0.997	0.999	1.002	1.000	1.005
	57.00	0.34082	0.00475	0.34527	0.997	1.000	1.002	1.000	1.002
	65.50	0.33512	0.00504	0.34112	0.998	1.000	1.003	1.000	1.002
0.225	37.50	0.31199	0.00658	0.31280	0.996	0.998	0.996	1.000	1.005
	43.00	0.30882	0.00631	0.30989	0.997	0.999	1.004	1.000	1.005
	49.50	0.31671	0.00659	0.31821	0.997	0.999	1.001	1.000	1.005
	57.00	0.30994	0.00435	0.31194	0.997	1.000	1.001	1.000	1.002
	65.50	0.31282	0.00470	0.31557	0.997	1.000	0.998	1.000	1.002
	75.00	0.30247	0.00499	0.30609	0.997	1.000	1.000	1.000	1.002
	86.00	0.30229	0.00533	0.30722	0.998	1.001	1.003	1.000	1.001
0.275	37.50	0.27396	0.00704	0.27435	0.997	0.999	0.997	1.000	1.005
	43.00	0.27856	0.00659	0.27909	0.997	1.000	1.000	1.000	1.005
	49.50	0.26652	0.00657	0.26720	0.997	1.000	0.997	1.000	1.005
	57.00	0.27485	0.00459	0.27580	0.997	1.000	0.995	1.000	1.002
	65.50	0.26066	0.00471	0.26187	0.997	1.000	1.004	1.000	1.002
	75.00	0.27476	0.00518	0.27649	0.997	1.001	1.004	1.000	1.002
	86.00	0.25960	0.00508	0.26182	0.998	1.001	1.000	1.000	1.002
	99.00	0.25794	0.00630	0.26097	0.998	1.001	0.998	1.000	1.000
	115.50	0.25851	0.00693	0.26278	0.998	1.001	0.998	1.000	1.000
0.35	43.00	0.20759	0.00472	0.20778	0.998	1.002	0.995	1.000	1.005
	49.50	0.21481	0.00480	0.21507	0.998	1.002	0.997	1.000	1.005
	57.00	0.21242	0.00329	0.21277	0.998	1.002	0.995	1.000	1.002
	65.50	0.20092	0.00333	0.20136	0.998	1.002	0.996	1.000	1.002
	75.00	0.20936	0.00360	0.20997	0.998	1.002	0.997	1.000	1.002
	86.00	0.20583	0.00358	0.20664	0.998	1.002	0.995	1.000	1.002
	99.00	0.20313	0.00375	0.20421	0.998	1.002	0.996	1.000	1.002
	115.50	0.20358	0.00441	0.20511	0.998	1.002	0.998	1.000	1.000
	137.50	0.20044	0.00472	0.20266	0.998	1.002	0.998	1.000	1.000
0.45	43.00	0.12927	0.00441	0.12933	1.003	1.011	0.989	1.000	1.005
	49.50	0.13776	0.00453	0.13784	1.002	1.010	0.989	1.000	1.005
	57.00	0.13211	0.00296	0.13221	1.001	1.009	0.994	1.000	1.002
	65.50	0.12867	0.00308	0.12880	1.001	1.008	0.996	1.000	1.002
	75.00	0.13325	0.00326	0.13342	1.000	1.007	0.998	1.000	1.002
	86.00	0.12660	0.00317	0.12682	1.000	1.006	0.996	1.000	1.002
	99.00	0.13142	0.00336	0.13172	0.999	1.006	0.998	1.000	1.002
	115.50	0.11975	0.00329	0.12014	0.999	1.005	0.996	1.000	1.001
	137.50	0.11797	0.00388	0.11853	0.999	1.005	0.999	1.000	1.000
	175.00	0.11841	0.00365	0.11937	0.998	1.004	0.998	1.000	1.000

0.55	43.00	0.07503	0.00349	0.07505	1.012	1.027	0.995	1.000	1.005
	49.50	0.07680	0.00348	0.07682	1.010	1.024	0.994	1.000	1.005
	57.00	0.07392	0.00221	0.07395	1.008	1.021	0.996	1.000	1.002
	65.50	0.06995	0.00234	0.06999	1.006	1.018	0.996	1.000	1.002
	75.00	0.07265	0.00258	0.07270	1.005	1.016	0.999	1.000	1.002
	86.00	0.06750	0.00247	0.06756	1.004	1.015	1.000	1.000	1.002
	99.00	0.06949	0.00262	0.06957	1.003	1.013	1.001	1.000	1.002
	115.50	0.06775	0.00263	0.06786	1.002	1.012	0.999	1.000	1.001
	137.50	0.07042	0.00324	0.07058	1.001	1.010	0.998	1.000	1.005
	175.00	0.05990	0.00273	0.06013	0.999	1.009	0.996	1.000	1.000
	230.00	0.06091	0.00366	0.06133	0.999	1.007	0.996	1.000	1.000
0.65	49.50	0.03371	0.00212	0.03372	1.027	1.051	1.032	1.000	1.005
	57.00	0.03359	0.00136	0.03360	1.022	1.045	1.025	1.000	1.002
	65.50	0.03077	0.00138	0.03078	1.018	1.039	1.016	1.000	1.002
	75.00	0.03236	0.00156	0.03237	1.015	1.035	1.012	1.000	1.002
	86.00	0.03091	0.00160	0.03092	1.012	1.031	1.009	1.000	1.001
	99.00	0.03182	0.00173	0.03184	1.010	1.027	1.007	1.000	1.001
	115.50	0.02900	0.00167	0.02902	1.007	1.024	1.007	1.000	1.001
	137.50	0.03160	0.00221	0.03164	1.005	1.021	1.006	1.000	1.000
	175.00	0.02724	0.00189	0.02729	1.002	1.017	1.008	1.000	1.000
	230.00	0.02965	0.00248	0.02975	1.000	1.014	1.007	1.000	1.000
0.75	57.00	0.01165	0.00077	0.01165	1.054	1.098	1.124	1.000	1.000
	65.50	0.01225	0.00087	0.01225	1.046	1.086	1.109	1.000	1.000
	75.00	0.01111	0.00091	0.01111	1.038	1.076	1.092	1.000	1.000
	86.00	0.00985	0.00088	0.00985	1.032	1.067	1.077	1.000	1.000
	99.00	0.01010	0.00098	0.01010	1.027	1.059	1.054	1.000	1.000
	115.50	0.00833	0.00093	0.00833	1.021	1.051	1.050	1.000	1.000
	137.50	0.00925	0.00106	0.00926	1.016	1.044	1.041	1.000	1.000
	175.00	0.00832	0.00098	0.00833	1.010	1.035	1.036	1.000	1.000
	230.00	0.00798	0.00130	0.00799	1.005	1.028	1.020	1.000	1.000

Figure captions

Fig. 1: $R = \sigma_L/\sigma_T$ measured in this experiment (BCDMS) as a function of x. Also shown is the measurement by the EMC on a hydrogen target [12]. Inner error bars are statistical only, outer error bars are statistical and systematic errors combined linearly. The solid line is the next-to-leading order QCD prediction using $\Lambda_{\overline{MS}} = 220$ MeV and a gluon distribution $xG(x,Q_0^2) = 4.5(1-x)^8$ at $Q_0^2 = 5$ GeV^2.

Fig. 2: The proton structure function $F_2(x,Q^2)$ measured at the four beam energies 100, 120, 200 and 280 GeV, using $R = R_{QCD}$. Only statistical errors are shown.

Fig. 3: The structure function $F_2(x,Q^2)$ from this experiment for all beam energies combined, using $R = R_{QCD}$. Also shown are data from the EMC [12] and SLAC-MIT [13] experiments which are rebinned to the x values of this experiment; note that there are no SLAC data in the lowest x bin. The relative normalizations between the experiments have not been adjusted. Only statistical errors are shown.

Fig. 4: The ratio of the proton structure functions $F_2(x)$ from this and from the EMC experiment [12]. In each bin of x, the data are averaged over the Q^2 range common to both measurements. Only statistical errors are shown.

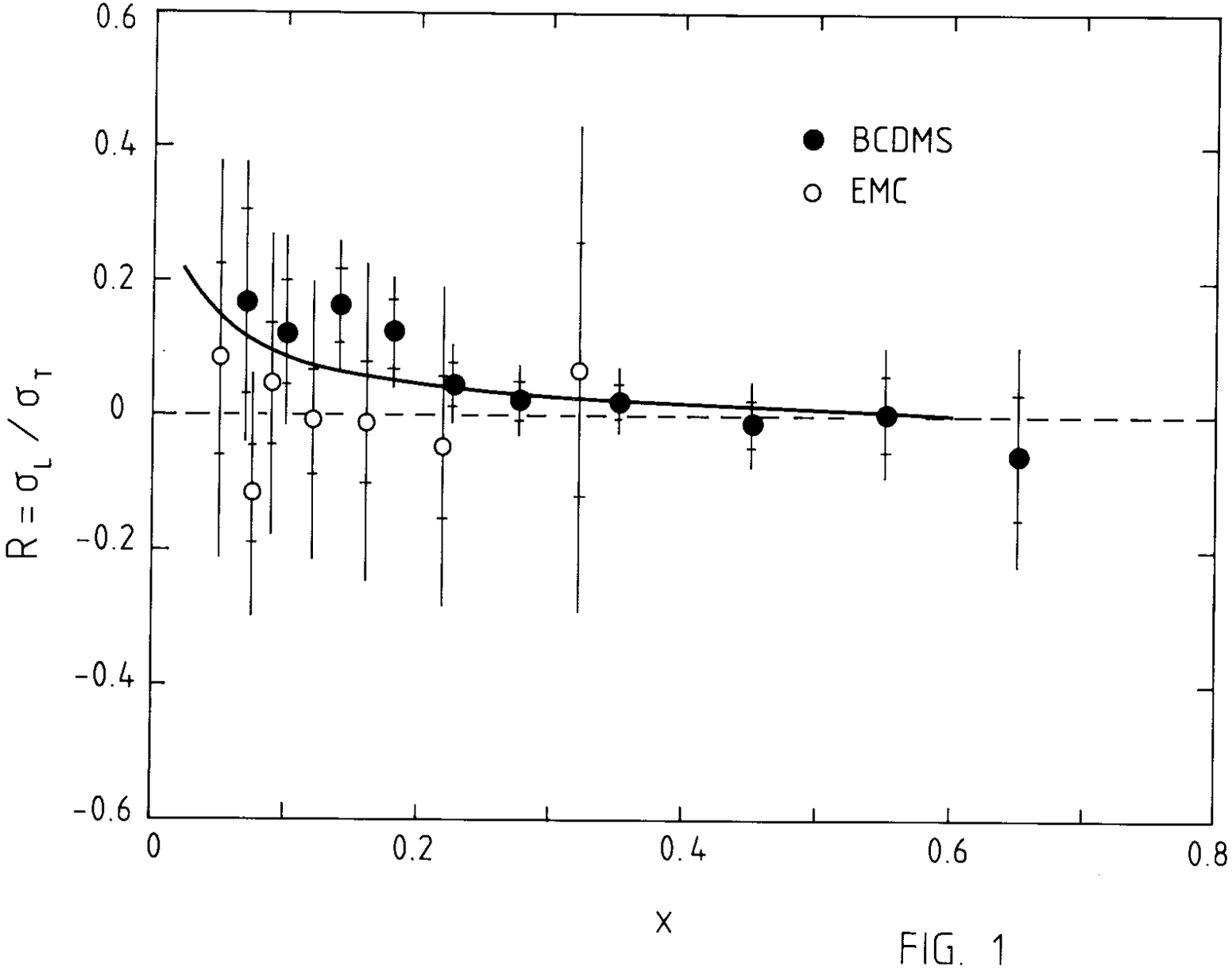

FIG. 1

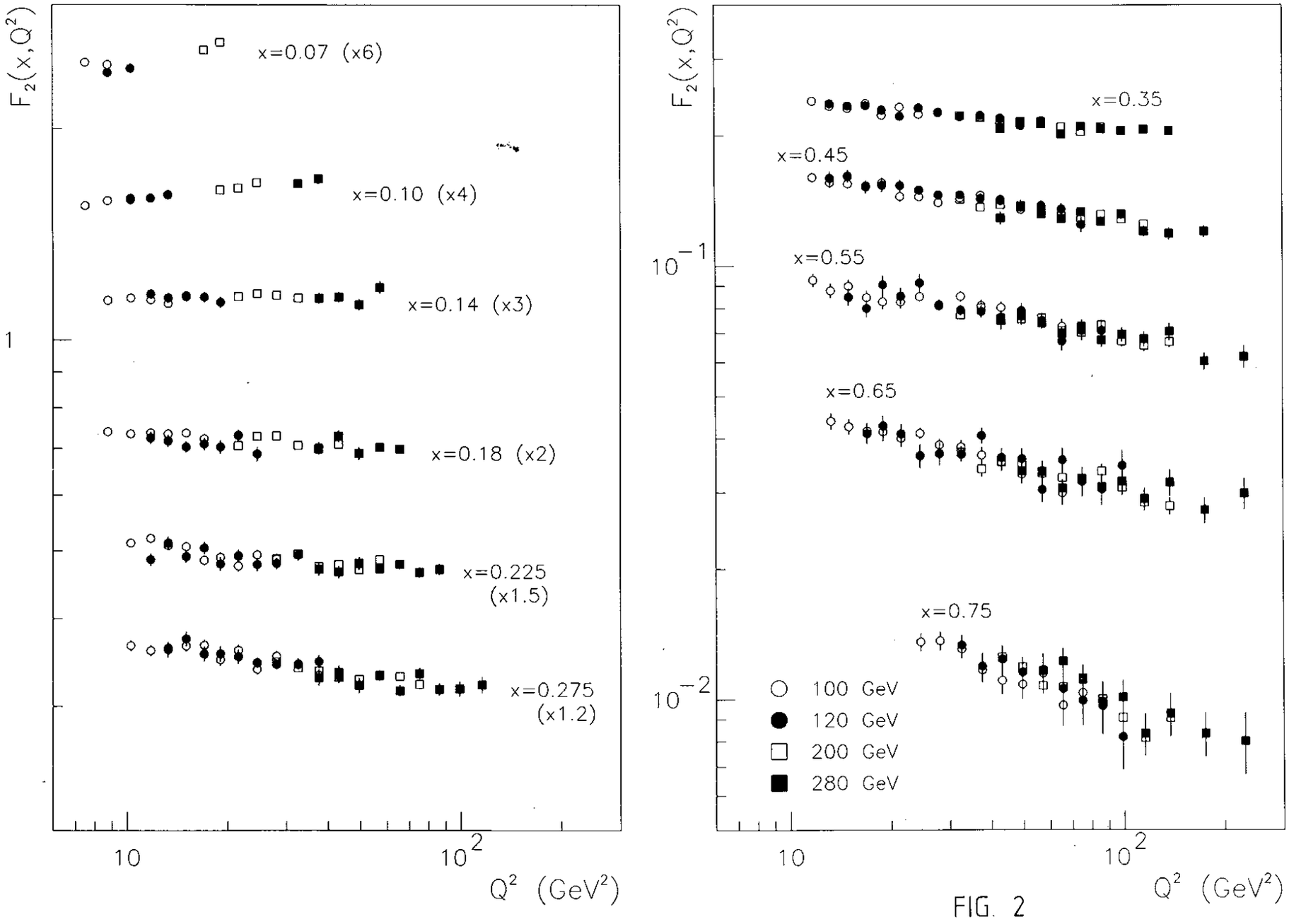
$F_2(x,Q^2)$
x=0.07 (x6)
x=0.10 (x4)
x=0.14 (x3)
x=0.18 (x2)
x=0.225
(x1.5)
x=0.275
(x1.2)
1
10
10^2
Q^2 (GeV^2)
$F_2(x,Q^2)$
x=0.35
x=0.45
x=0.55
x=0.65
x=0.75
10^{-1}
10^{-2}
100 GeV
120 GeV
200 GeV
280 GeV
10
10^2
Q^2 (GeV^2)

FIG. 2

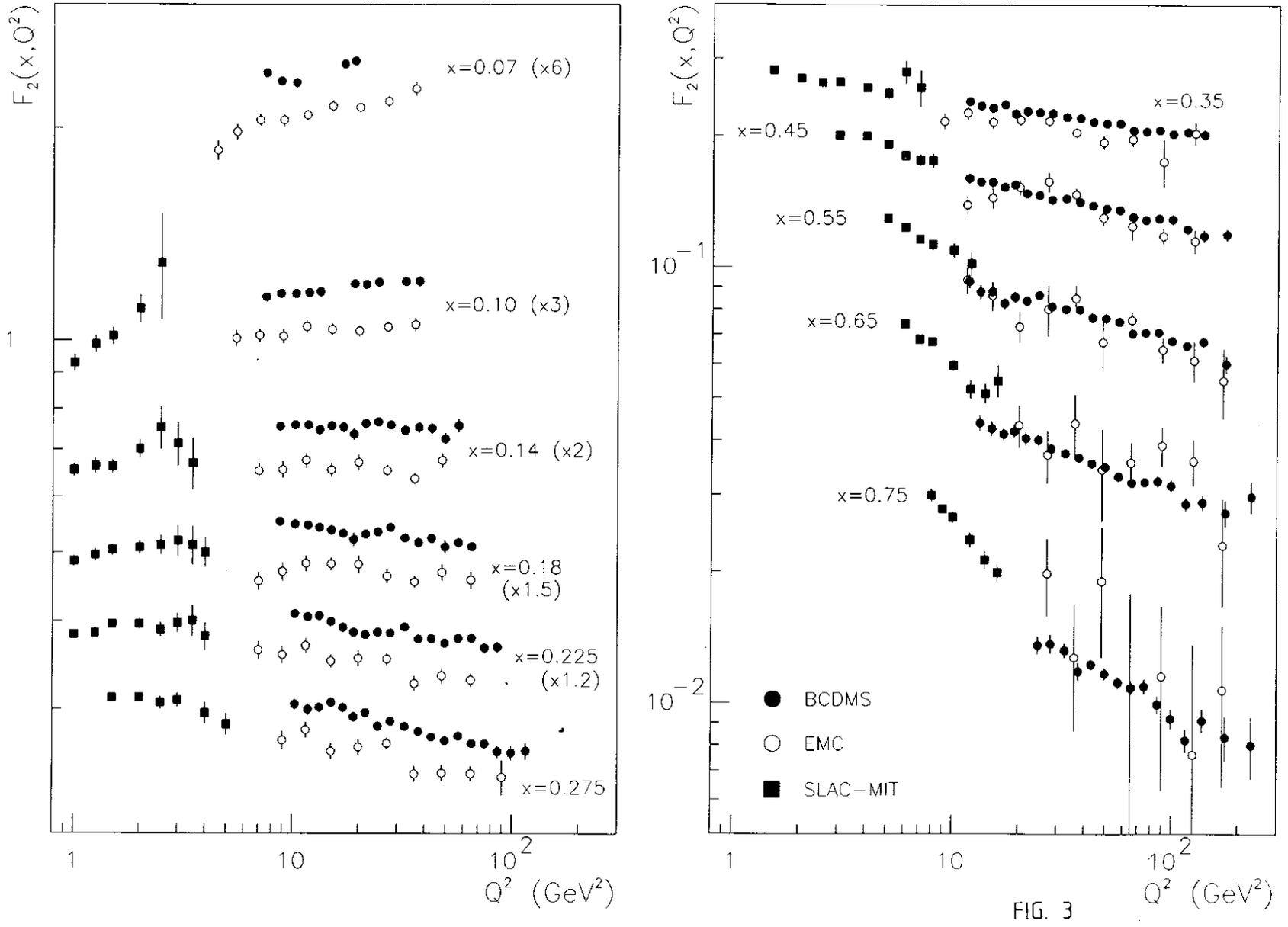
$F_2(x,Q^2)$
x=0.07 (x6)
x=0.10 (x3)
x=0.14 (x2)
x=0.18 (x1.5)
x=0.225 (x1.2)
x=0.275
1
10
10^2
Q^2 (GeV^2)
$F_2(x,Q^2)$
x=0.35
x=0.45
x=0.55
x=0.65
x=0.75
10^{-1}
10^{-2}
BCDMS
EMC
SLAC–MIT
1
10
10^2
Q^2 (GeV^2)

FIG. 3

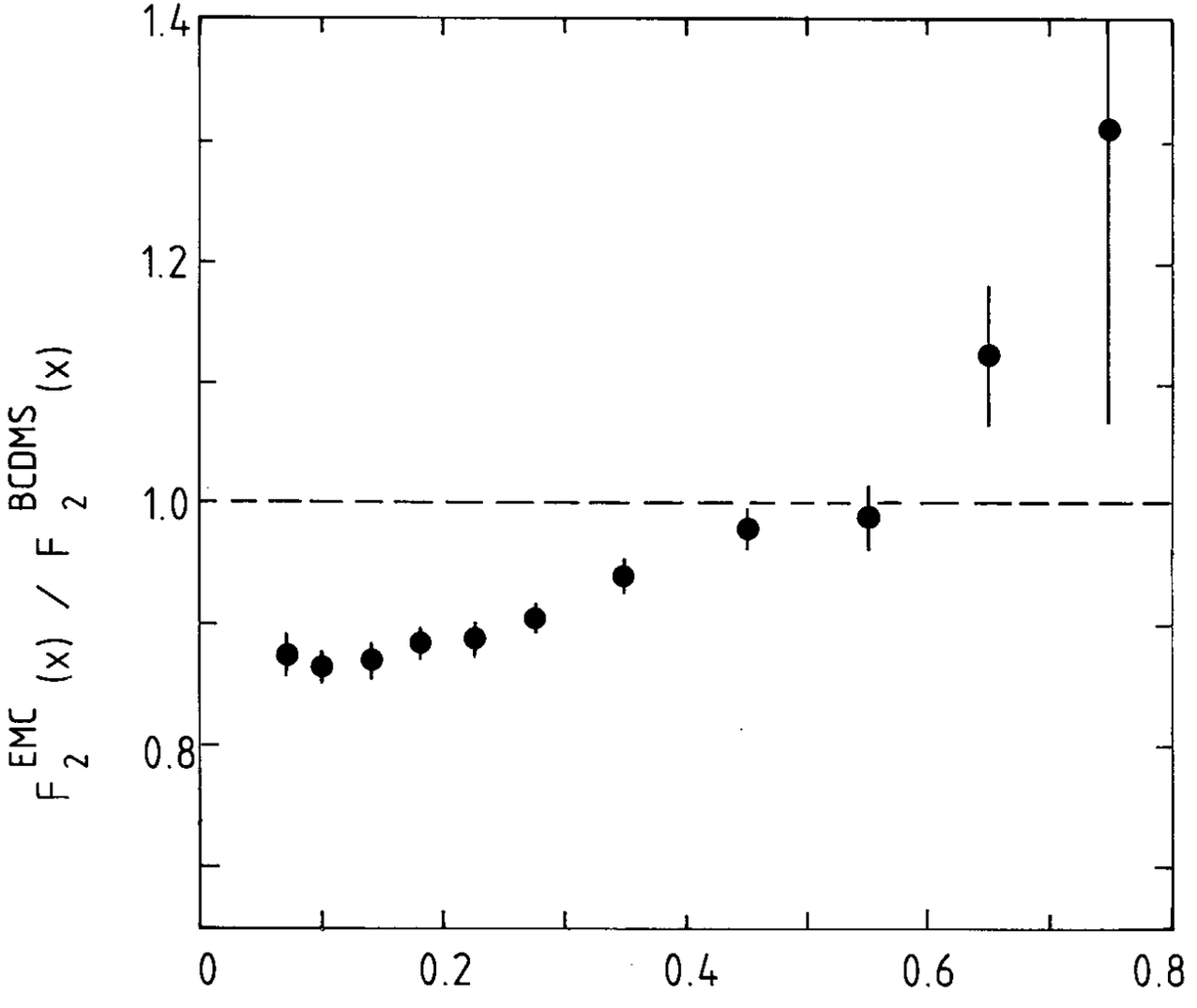

Fig. 4